

We are IntechOpen, the world's leading publisher of Open Access books Built by scientists, for scientists

6,900

Open access books available

186,000

International authors and editors

200M

Downloads

Our authors are among the

154

Countries delivered to

TOP 1%

most cited scientists

12.2%

Contributors from top 500 universities



WEB OF SCIENCE™

Selection of our books indexed in the Book Citation Index
in Web of Science™ Core Collection (BKCI)

Interested in publishing with us?
Contact book.department@intechopen.com

Numbers displayed above are based on latest data collected.
For more information visit www.intechopen.com



Investigation of Lattice Defects in GaAsN Grown by Chemical Beam Epitaxy Using Deep Level Transient Spectroscopy

Boussairi Bouzazi¹, Hidetoshi Suzuki², Nobuaki Kijima¹,
Yoshio Ohshita¹ and Masafumi Yamaguchi¹

¹Toyota Technological Institute

²Myazaki University
Japan

1. Introduction

With only 3 % of N and 9 % of In, InGaAsN with a band gap of 1.04 eV was obtained and could be lattice matched to GaAs and Ge. This dilute nitride semiconductor has been selected as a promising candidate for high efficiency multijunction tandem solar cells (Geisz and Friedman, 2002). However, the diffusion length of minority carriers and the mobility are still lower than that in GaAs or InGaAs and showed a considerable degradation with increasing the N concentration. These electrical properties are insufficient to insure the current matching in the multijunction solar cell structure AlInGaP/GaAs/InGaAsN/Ge (Friedman et al., 1998). An obvious reason of such degradation is the high density of N-related lattice defects that can be formed during growth to compensate for the tensile strain caused by the small atomic size of N compared with that of arsenic (As) and to the large miscibility of the gap between GaAs and GaN. These defect centers are expected to act as active recombination and/or scattering centers in the forbidden gap of the alloy (Zhang & Wei, 2001). However, no experimental evidence has yet been reported. On the other hand, the conductivity of undoped *p*-type InGaAsN or GaAsN and their high background doping (Friedman et al., 1998; Kurtz et al., 1999; Moto et al., 2000; Krispin et al., 2000) prevent the design of wide depletion region single junction solar cell and the fabrication of intrinsic layer to overcome the short minority carrier lifetime. This serious problem was expected in the first stage to the density of unintentional carbon in the film (Friedman et al., 1998; Kurtz et al., 1999; Moto et al., 2000). However, the carrier density in some InGaAsN semiconductors was found to be higher than that of carbon (Kurtz et al., 2002). Furthermore, the high density of hydrogen (up to 10^{20} cm⁻³) and the strong interaction between N and H in InGaAsN to form N-H related complex were confirmed to be the main cause of high background doping in InGaAsN films (Li et al., 1999; Janotti et al., 2002, 2003; Kurtz et al., 2001, 2003; Nishimura et al., 2007). In addition, N-H complex was found theoretically to bind strongly to gallium vacancies (V_{Ga}) to form N-H- V_{Ga} with a formation energy of 2 eV less than that of isolated V_{Ga} (Janotti et al., 2003). These predictions were supported experimentally using positron annihilation spectroscopy results (Toivonen et al., 2003).

On the other hand, similar electrical properties were obtained in InGaAsN grown by metal-organic chemical vapor deposition (MOCVD) and molecular beam epitaxy (MBE) despite the large difference in the density of residual impurities, which excludes them as a main cause of low mobilities and short minority carrier lifetimes. For that, lattice defects, essentially related to the N atom, were expected to be the main reason of such degradation. Several theoretical and experimental studies have investigated carrier traps in InGaAsN films. Theoretically, using the first principles pseudo-potential method in local density approximation, four N-related defects were proposed: $(\text{As}_{\text{Ga}}\text{-N}_{\text{As}})_{\text{nr}}$, $(\text{V}_{\text{Ga}}\text{-N}_{\text{As}})_{\text{nr}}$, $(\text{N-N})_{\text{As}}$, and $(\text{N-As})_{\text{As}}$ (Zhang & Wei, 2001). While the two first structures were supposed to have lower formation probabilities, the two split interstitials $(\text{N-N})_{\text{As}}$ and $(\text{N-As})_{\text{As}}$ were suggested to compensate the tensile strain in the film and to create two electron traps at around 0.42 and 0.66 eV below the conduction band minimum (CBM) of InGaAsN with a band gap of 1.04 eV, respectively (Zhang & Wei, 2001). Experimentally, the ion beam analysis provided a quantitative evidence of existence of N-related interstitial defects in GaAsN (Spruytte et al., 2001; Ahlgren et al., 2002; Jock, 2009). Furthermore, several carrier traps were observed in GaAsN and InGaAsN using deep level transient spectroscopy (DLTS). A deep level (E2/H1), acting as both an electron and a hole trap at 0.36 eV below the CBM, was observed (Krispin et al., 2001). Other electron traps in GaAsN grown by MBE were recorded: A2 at 0.29 eV and B1 at 0.27 eV below the CBM of the alloy (Krispin et al., 2003). In addition, a well known electron trap at 0.2 ~ 0.3 eV and 0.3 ~ 0.4 eV below the CBM of *p*-type and *n*-type GaAsN grown by MOCVD were observed, respectively (Johnston et al., 2006). Although the importance of these results as a basic knowledge about lattice defects in GaAsN and InGaAsN, no recombination center was yet experimentally proved and characterized. Furthermore, the main cause of high background doping in *p*-type films was not completely revealed.

Chemical beam epitaxy (CBE) has been deployed (Yamaguchi et al., 1994; Lee et al., 2005) to grow (In)GaAsN in order to overcome the disadvantages of MOCVD and MBE. It combines the use of metal-organic gas sources and the beam nature of MBE. (In)GaAsN films were grown under low pressure and low temperature to reduce the density of residual impurities and to avoid the compositional fluctuation of N, respectively. Furthermore, a chemical N compound source was used to avoid the damage of N species from N_2 plasma source in MBE. Although we obtained high quality GaAsN films grown by CBE, the diffusion length of minority carriers is still short (Bouzazi et al., 2010). This indicates that the electrical properties of GaAsN and InGaAsN films are independent of growth method and the problem may be caused by the lattice defects caused by N. Therefore, it is necessary to investigate these defects and their impact on the electrical properties of the film. For that, this chapter summarizes our recent results concerning lattice defects in GaAsN grown by CBE. Three defect centers were newly obtained and characterized. The first one is an active non-radiative N-related recombination center which expected to be the main cause of short minority carrier lifetime. The second lattice defect is a N-related acceptor like-state which greatly contributes in the background doping of *p*-type films. The last one is a shallow radiative recombination center acceptor-like state.

2. Deep level transient spectroscopy

To characterize lattice defects in a semiconductor, several techniques were used during the second half of the last century. Between these methods, we cite the thermally stimulated

current (TSC) (Leonard & Grossweiner, 1958; Bube, 1960), the admittance spectroscopy (Losee, 1974), the increase or decay curves of photoconductivity (Rose, 1951; Devore, 1959), the optically stimulated conductivity (Lambe, 1955; Bube, 1956), and the analysis of space-charge-limited currents as function of applied voltage (Smith & Rose, 1955; Rose, 1955; Lampert, 1956). The basic concept of using the change of capacitance under bias conditions by the filling and emptying of deep levels was already anticipated fifty years ago (Williams, 1966). The thermally stimulated capacitance (TSCAP), which gives the temperature dependence of junction capacitance (Sah et al., 1978; Sah & Walker, 1973), was used. By dressing the properties of all these techniques, D. V. Lang found that they lacked the sensitivity, the speed, the depth range of recorded trap, and the spectroscopic nature to make them practical for doing spectroscopy on non-radiative centers. For that, in 1974, he proposed DLTS as a characterization method of lattice defects that can overcome the disadvantages of the other methods (Lang, 1974). DLTS is based on the analysis of the change of capacitance due to a change in bias condition at different temperatures. It can be applied to Schottky contacts and p - n junctions. DLTS has advantages over TSC due to its better immunity to noise and surface channel leakage currents. It can distinguish between majority and minority carrier traps, unlike TSC, and has a strong advantage over admittance spectroscopy, which is limited to majority-carrier traps. Comparing with TSCAP, DLTS has much greater range of observable trap depths and improved sensitivity. Despite the success of optical techniques such as photoluminescence to characterize superficial levels, they are rarely used in the study of non-radiative deep levels. Furthermore, such experiences must be done in the infrared domain. However, sensors are less sensitive than in the visible domain. Thus, we need a technique, which can separate between minority and majority traps and evaluate their concentrations, their energies, and their capture cross sections.

2.1 Fundamental concept of DLTS

2.1.1 Capacitance transient

To fully understand DLTS, it is worth to have a basic knowledge of capacitance transients arising from the SCR of Schottky contacts or p^+n/n^+p asymmetric junctions. If a pulse voltage is applied to one of these device structures that is originally reverse-biased, the SCR width decreases and the trap centers are filled with carriers (majority or minority depending on the structure). When the junction is returned to reverse bias condition, the traps that remains occupied with carriers are emptied by thermal emission and results in a transient decay. The capacitance transients provide information about these defect centers. Here, we restrain our description to a p^+n junction where the p -side is more much heavily doped than the n -side, which gives the SCR almost in the low doped side.

The causes of change in capacitance depend on the nature of applied voltage. In case of reverse biased voltage, the junction capacitance, due to the change in SCR width, is dominant. However, when the applied voltage is forward biased, the diffusion capacitance, due to the contribution of minority carrier density, is dominant. The basic equation governing the capacitance transient in the p^+n junction is expressed by

$$C(t) = A \sqrt{\frac{\epsilon \epsilon_0 e N_D}{2(V_R + V_b)}} \left[1 - \frac{N_T}{2N_D} \exp\left(-\frac{t}{\tau}\right) \right] = C_0 \left[1 - \frac{N_T}{2N_D} \exp\left(-\frac{t}{\tau}\right) \right] \quad (1)$$

where A is the contact area, V_b is the built-in potential, $\epsilon \epsilon_0$ is the permittivity of the semiconductor material, and e is the elementary charge of an electron. C_0 , N_T , N_D , and τ

denote the junction capacitance at reverse bias, the density of filled traps under steady state conditions, the ionized donor concentration, and the time constant that gives the emission rate, respectively. The change in capacitance after the recharging of traps is given by

$$\Delta C = C_0 \sqrt{1 - \frac{N_T}{N_D}} \quad (2)$$

In most cases of using transient capacitance, the trap centers form only a small fraction of the SCR impurity density, i.e., $N_T \ll N_D$. Hence, using a first-order expansion of Eq. (2) gives

$$|\Delta C| = C_0 |1 - N_T/2N_D| \cong C_0 N_T/2N_D \quad (3)$$

Thus, the trap concentration calculates from the capacitance change ΔC is expressed by

$$N_T = 2 \frac{\Delta C}{C_0} N_D \quad (4)$$

Note that Eq. (3) assumes that $N_T \ll N_D$ and the traps are filled throughout the total depletion width. To be more accurate, N_T should be adjusted to N_{Tadj} according to [30]

$$N_{Tadj} = 2 \frac{\Delta C}{C_0} N_D \frac{W_R^2}{L_1^2 - L_2^2} \quad (5)$$

where W_R is the total SCR at reverse bias voltage V_R , $L_1 = W_R - \lambda$, $L_2 = W_p - \lambda$, and

$$\lambda = \left(\frac{2\epsilon\epsilon_0}{e^2 N_D} (E_F - E_T) \right)^{1/2} \quad (6)$$

where W_p , E_F , and E_T denote the SCR at V_p , the Fermi level, and the trap energy level.

2.1.2 Thermal emission of carriers from deep levels

The emission rates for electrons and holes are given, respectively by

$$e_n = \sigma_n v_{thn} N_c \exp\left(-\frac{E_{CBM} - E_T}{kT}\right) \quad (7)$$

$$e_p = \sigma_p v_{thp} N_v \exp\left(-\frac{E_T - E_{VBM}}{KT}\right) \quad (8)$$

where σ_n , N_c , and v_{thn} are the thermal capture cross section, the density of states, and the thermal velocity of holes, respectively. σ_p , N_v , and v_{thp} are the same parameters for holes. E_{CBM} , E_{VBM} , and E_T are the energy levels of the conduction band minimum, the valence band maximum, and the trap, respectively.

2.2 Other DLTS related techniques

The isothermal capacitance transient spectroscopy (ICTS) and the double carrier pulse DLTS (DC-DLTS) are two DLTS related methods. They are used to obtain the density profiling of lattice defects and to check whether they act as recombination centers or not, respectively.

2.2.1 Isothermal capacitance transient spectroscopy

ICTS is used to analyze the profiling of lattice defects in the SCR of the semiconductor. It can be done through three different methods. The first one is obtained by fixing V_R and varying V_p to build difference of transients among the SCR of the device. The second method is evaluated by measuring at constant V_p and varying V_R . The last option is obtained by varying V_R and V_p , where the profiling analysis is also possible without building difference of transients. Using the first method, the medium trap density $\bar{N}_T(x_{ij})$ at a point x_{ij} is given by

$$\bar{N}_T(x_{ij}) = \frac{2 N_D (\epsilon \epsilon_0)^2 A^2 \Delta C_{ij}}{C_R^3 (L_{p_i}^2 - L_{p_j}^2)} \quad (9)$$

where ΔC_{ij} is the amplitude difference of the two capacitance transients.

2.2.2 Double carrier pulse DLTS

DC-DLTS is used in asymmetric n^+p or p^+n junctions (Khan et al., 2005). It aims to check whether a trap is a recombination center or not. As shown in Fig. 1, two pulsed biases are applied to the sample, in turn, to inject majority and minority carriers to an electron trap. At the initial state, the junction is under reverse bias, and the energy level E_T of the trap is higher than the Fermi level (E_{Fn}). When the first pulse voltage is applied to the sample, E_{Fn} is higher than E_T , which allows the trap to capture electrons. During the second reverse biased pulse, with a duration t_{ip} , holes are injected to the SCR from the p -side of the junction. After the junction pulse is turned off, electrons and holes are thermally emitted. The amount of trapped carriers can be observed as a change in the DLTS peak height of the trap. If the trap captures both electrons and holes, the DLTS maximum of the corresponding level decreases compared with that in conventional DLTS. Such a decrease is explained by the electron-hole ($e-h$) recombination process, which indicates that the level is a recombination center.

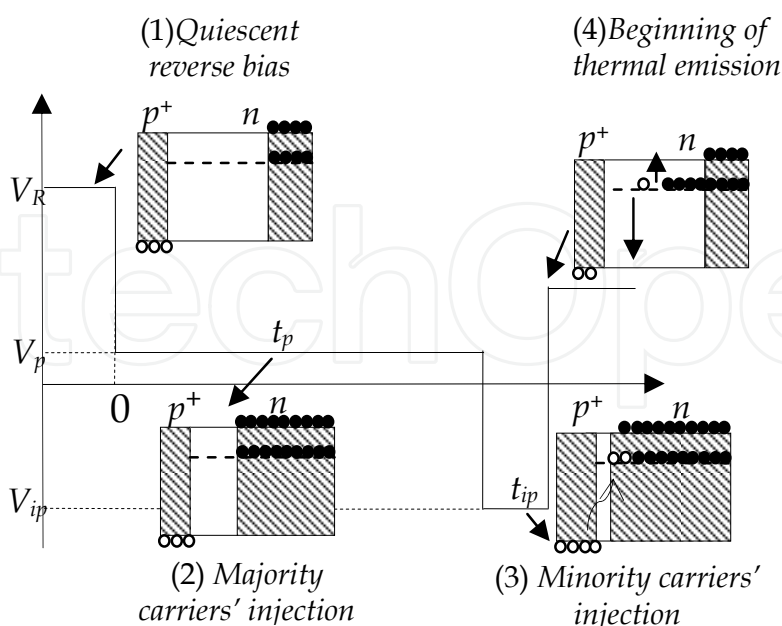


Fig. 1. Basic concept of capture and thermal emission processes from an electron trap located at an energy level E_T in p^+n junction. A saturating injection pulse is applied to the reverse biased junction to fill the trap with holes.

To formulate the recombination process, we consider the same notation in § 2.1.2, with assuming that $n \approx N_D$. The relationship between the total density of recombination centers and that only occupied by electrons in the n-side of the junction can be expressed by

$$\frac{dn_T}{dt} = -e_p n_T(t) + \langle p \rangle c_p [N_T - n_T(t)] - N_D c_n n_T(t) + e_n [N_T - n_T(t)] \quad (10)$$

where $\langle p \rangle$ is the average of injected holes. As a solution of Eq. (10), we have

$$\frac{dn_T}{dt} = n_T(t_{ip}) = n_T(\infty) + [n_T(0) - n_T(\infty)] \exp\left(-\frac{t_{ip}}{\tau}\right) \quad (11)$$

where $n_T(\infty) = (\langle p \rangle c_p + e_n) / (\tau^{-1} N_T)$, $\tau^{-1} = \langle p \rangle c_p + N_D c_n + e_n + e_p$, and t_{ip} is the width of the injected pulse. Considering the I_{DLTS} and $I_{DC-DLTS}$ the peak heights of the recombination center in conventional and DC-DLTS, respectively. Equation (11) can be rewritten properly as

$$\frac{n_T(t_{ip})}{N_T} = \frac{(I_{DLTS} - I_{DCDLTS})}{I_{DCDLTS}} = \langle p \rangle \sigma_p v_{thp} t_{ip} \quad (12)$$

Similarly for hole trap in the p -side of a n^+p junction, which acts as recombination center, we obtain

$$\frac{n_T(t_{ip})}{N_T} = \frac{(I_{DLTS} - I_{DCDLTS})}{I_{DCDLTS}} = \langle n \rangle \sigma_n v_{thn} t_{ip} \quad (13)$$

where $\langle n \rangle$ is the average of injected electrons.

3. Experimental procedure

All GaAsN films were grown by CBE on high conductive n - or p -type GaAs 2° off toward [010] substrate using Triethylgallium ($(C_2H_5)_3Ga$, TEGa), Trisdimethylaminoarsenic ($[(CH_3)_2N]_3As$, TDMAAs), and Monomethylhydrazine ($CH_3N_2H_3$, MMHy) as Ga, As, and N sources, respectively. The flow rates TEGa = 0.1 sccm and TDMAAs = 1.0 sccm were considered as conventional values. The growth temperatures of 420 °C and 460 °C were used for p -type and n -type GaAsN, respectively. Concerning the doping, p -type GaAsN films are unintentionally doped. The n -type alloys were obtained using a silane (SiH_4) source or by growing the films under lower MMHy and high growth temperature.

Three different device structures are used in this study: (i) n - and p -type GaAsN schottky contacts, (ii) n^+ -GaAs/ p -GaAsN/ p -GaAs, and (iii) n -GaAsN/ p^+ -GaAs hetero-junctions. The N concentration in all GaAsN layers was evaluated using XRD method. Aluminum (Al) dots with a diameter of 0.5/1 mm were evaporated under vacuum on the surface of each sample. Alloys of Au-Ge (88:12 %) and Au-Zn (95:05 %) were deposited at the bottom of n -type and p -type GaAs substrates for each device, respectively. Some samples were treated by post-thermal annealing under N_2 liquid gas and using GaAs cap layers to avoid As evaporation from the surface. The temperature and the time of annealing will be announced depending on the purpose of making annealing. The background doping and the doping profile in the extended depletion region under reverse bias condition were evaluated using the capacitance-voltage (C-V) method. The leakage current in all used samples ranged from 0.3

nA to $10 \mu A$ for a maximum reverse bias voltage of $-4 V$. A digital DLTS system *Bio-Rad DL8000* was used for DLTS and C-V measurements. The activation energy E_t and the capture cross section $\sigma_{n,p}$ were determined from the slope and the intercept values of the Arrhenius plot, respectively.

4. Lattice defects in GaAsN grown by CBE

In this section, the distribution of electron and hole traps in the depletion region of GaAsN grown by CBE will be dressed using DLTS and related methods.

4.1 Electron traps in GaAsN grown by CBE

4.1.1 DLTS spectra and properties of a N-related electron trap

The DLTS spectrum of Fig. 2(a) shows an electron trap ($E2$) at $0.69 eV$ below the CBM of GaAs. After rapid thermal annealing at $720^\circ C$ for 2 min, $E2$ disappears completely whereas a new electron trap ($E3$) appears at $0.34 eV$ below the CBM. From the Arrhenius plots of Fig. 2(d), the capture cross sections of $E2$ and $E3$ are calculated to be $\sigma_{E2} = 8.1 \times 10^{-15} cm^2$ and $\sigma_{E3} = 7.5 \times 10^{-18} cm^2$, respectively. Based on previous results about native defects in n -type GaAs, $E2$ and $E3$ are independent of N and considered to be identical to $EL2$ and $EL3$, respectively (Reddy et al., 1996). In order to focus only on N -related lattice defects, these two energy levels will be excluded from the DLTS spectra of N -containing n -type GaAsN. The addition

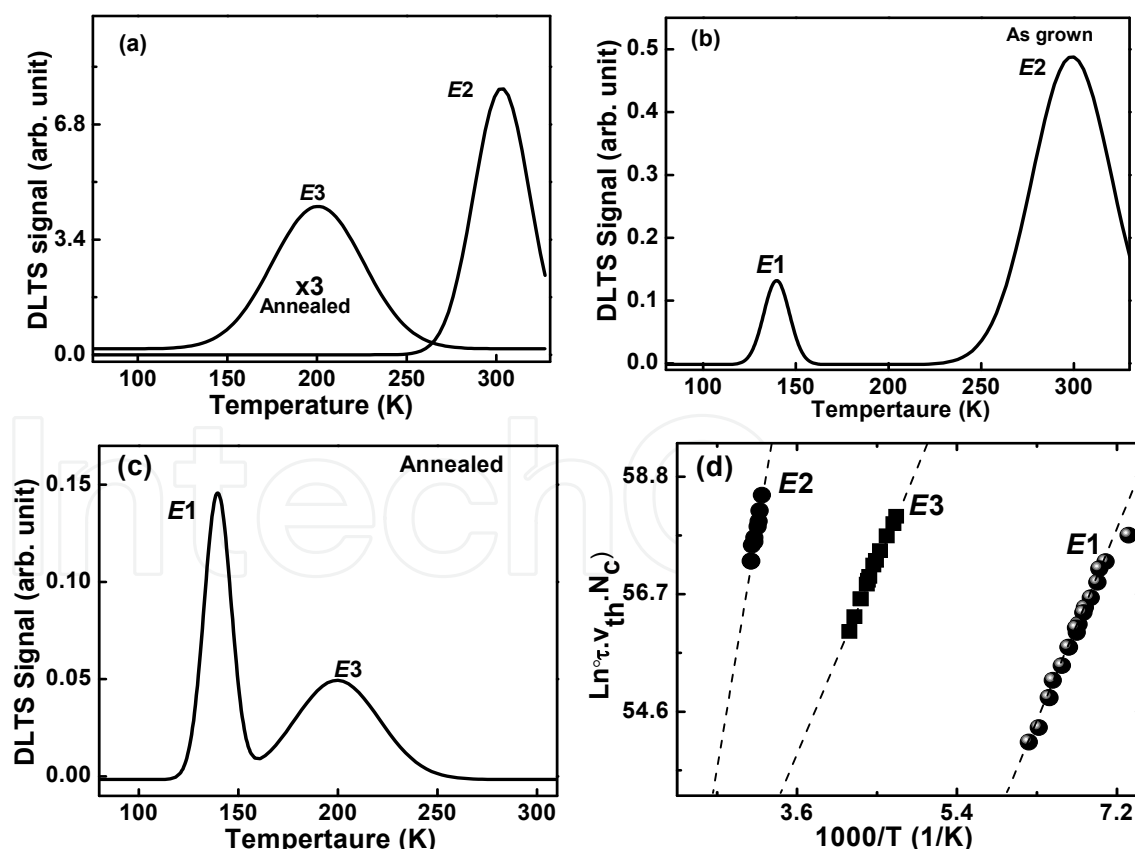


Fig. 2. DLTS spectra of (a) N free as grown and annealed GaAs, (b) as grown n -type $GaAs_{0.998}N_{0.002}$, (c) annealed n -type $GaAs_{0.998}N_{0.002}$, and (d) Arrhenius plots of DLTS spectra.

of a small atomic fraction of N to GaAs leads to the record of a new electron trap ($E1$), at an average activation energy 0.3 eV below the CBM of GaAsN. The DLTS spectra of as grown and annealed n -type GaAs_{0.998}N_{0.002} are given in Figs. 2. (b) and (c), respectively. The activation energies (E_{E1}) and the capture cross sections (σ_{E1}) of $E1$ for N varying GaAsN samples are given Fig. 3 (a) and (b), respectively. The fluctuation of E_{E1} from one sample to another can be explained by the effect of Poole–Frenkel emission, where the thermal emission from $E1$ is affected by the electric field (Johnston and Kurtz, 2006). As illustrated in Fig. 3(c), with increasing the filling pulse duration, the DLTS peak height of $E1$ saturates

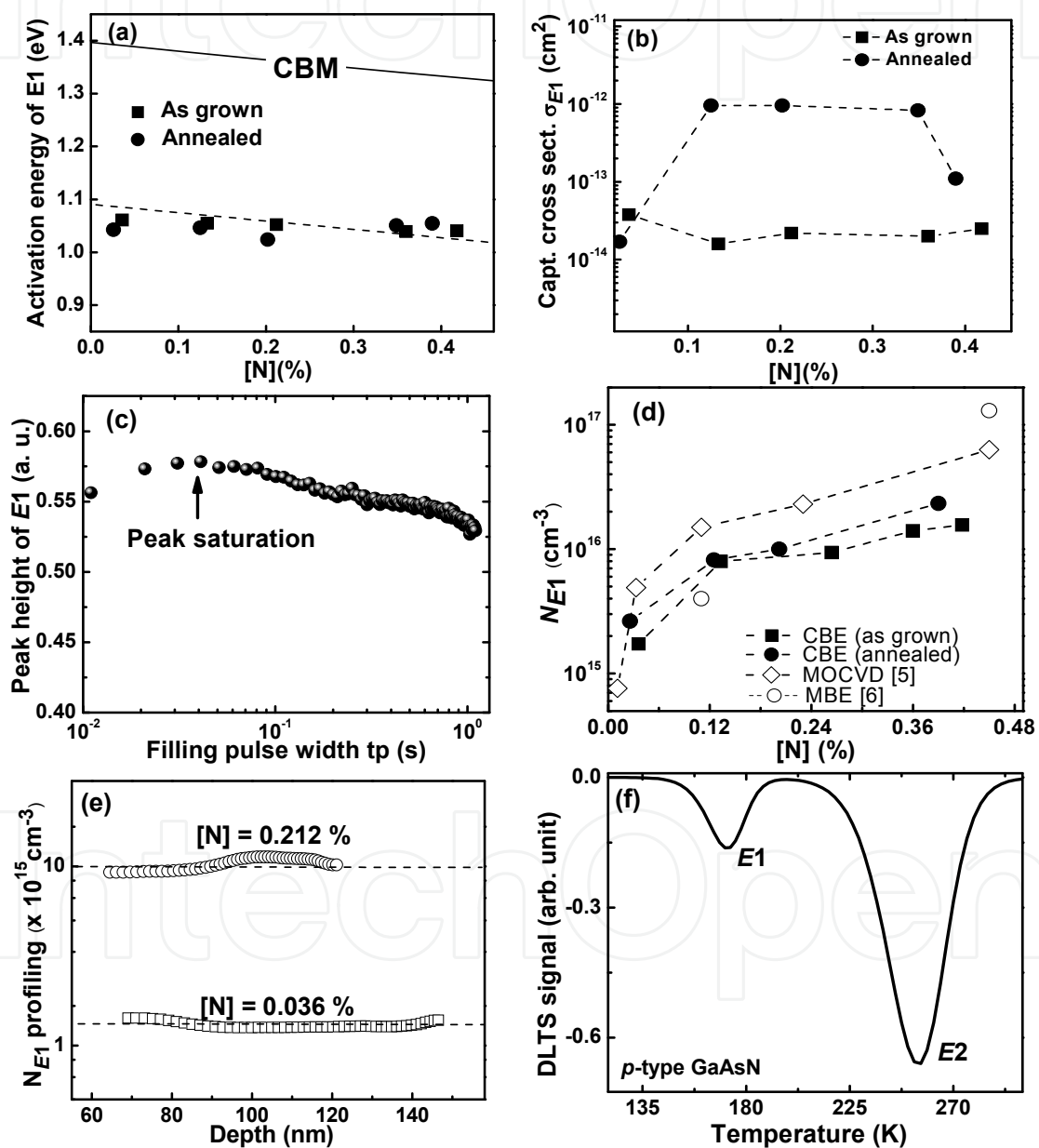


Fig. 3. Nitrogen dependence of (a) thermal activation energy, (b) capture cross section, and (d) adjusted density of $E1$ in as grown and annealed GaAsN samples. The large capture cross section is confirmed with (c) the filling pulse width dependence of the DLTS peak height of $E1$. (e) Density profiling of $E1$ in the bulk of GaAsN films, and (f) DLTS spectrum of undoped p -type GaAsN grown by CBE.

rapidly. This behavior is explained by the large value of σ_{E1} , compared with that of $E2$, $E3$, and other native defects in GaAs. The adjusted densities of $E1$ (N_{E1}) in as grown and annealed samples are plotted in Fig. 3(d). N_{E1} increases considerably with increasing $[N]$ in the film and persists to post thermal annealing. This indicates that $E1$ is a N -related and a stable electron trap.

The defect center $E1$ was not observed previously in N free GaAs grown by CBE despite the existence of N species in the chemical composition of the As source. This can be explained through three possible scenarios. First, the absence of tensile strain in GaAs prevents the formation of $E1$. Second, the N atom in the atomic structure of $E1$ comes from the N source. Finally, the N atom comes from the N and As compound sources and in presence of tensile strain $E1$ can be formed. The tensile strain was reported in most theoretical and experimental studies. As given in Fig. 3(e) and using the ICTS, this idea is supported by the uniform distribution of N_{E1} in the bulk of GaAsN. This indicates that $E1$ is formed during growth to compensate for the tensile strain in the GaAsN films caused by the small atomic size of N compared with that of As.

Furthermore, the properties of $E1$ are identical to that of the famous electron traps reported by Johnston et Kurtz (Johnston and Kurtz, 2006) and Krispin et al. (Krispin et al., 2003) in MOCVD and MBE grown n -type GaAsN, respectively. As illustrated in Fig. 3(d), the densities of these traps are approximately similar to N_{E1} despite the large difference in the density of residual impurities between the three growth methods. Therefore, the atomic structure of $E1$ may be free from impurities. Furthermore, by carrying out DLTS measurements for minority carriers in undoped p -type film, $E1$ was also observed. This indicates clearly that $E1$ is independent of doping atoms (see Fig. 3(f)).

4.1.2 Nature of the electron trap E1

Two methods are used to verify whether $E1$ is a recombination center or not. The first method is indirect, in which the activation energy of deep levels is correlated with that of the reverse bias current in the depletion region of n -type GaAsN Schottky junction and n^+ -GaAs/ p -GaAsN heterojunction. These two device structures are selected because the current is due mainly to electrons. The second method is direct, in which DC-DLTS is used to show the behavior of the electron traps in simultaneous injection of majority and minority carriers in the depletion region.

4.1.2.1 Origin of reverse bias current in GaAsN

The temperature dependence of the reverse bias current in the depletion region of n -type GaAsN Schottky junction and n^+ -GaAs/ p -GaAsN is shown in Fig. 4(a) for reverse bias voltages of 0.5 and -0.5 V, respectively. At lower temperature, the dark current changes slowly in the two structures, then follows an Arrhenius type behavior. As shown in Fig. 4(b), the same result is obtained by applying reverse bias voltages of 1 and -1 V. Under these conditions, the reverse bias current $I_d(T)$ can be expressed by

$$I_d(T) = I_\infty \exp\left(-\frac{\Delta E}{kT}\right) \quad (14)$$

where I_∞ , ΔE , k , and T denote the limit of the high-temperature current, the thermal activation energy of the reverse bias current, the Boltzmann constant, and the temperature, respectively. The I-V characteristics deviate in the two samples from the thermionic emission. This is

explained by the fact that supplying the p - n junction under reverse bias conditions decreases the product of excess carriers to less than the square of intrinsic carriers. Hence, the Shockley-Read-Hall (SRH) generation mechanism is activated to increase the product of excess carriers to assure the balance of charge. The generated carriers are swept to the transition regions by the electric field in the depletion region. Therefore, an SRH center, with a thermal activation energy around 0.3 eV, is the origin of the dark current in the SCR of GaAsN. The thermal activation energies are measured with respect to majority and minority carriers in n -type GaAsN schottky junction and n^+ -GaAs/ p -GaAsN heterojunction, respectively. This corresponds to the conduction band in the two structures. By correlating the conduction mechanism and DLTS measurements, the thermal activation energy of the reverse bias current and the activation energy of the N -related electron trap $E1$ are typically identical. Therefore, $E1$ is responsible for the generation/recombination current in the depletion region of GaAsN grown by CBE.

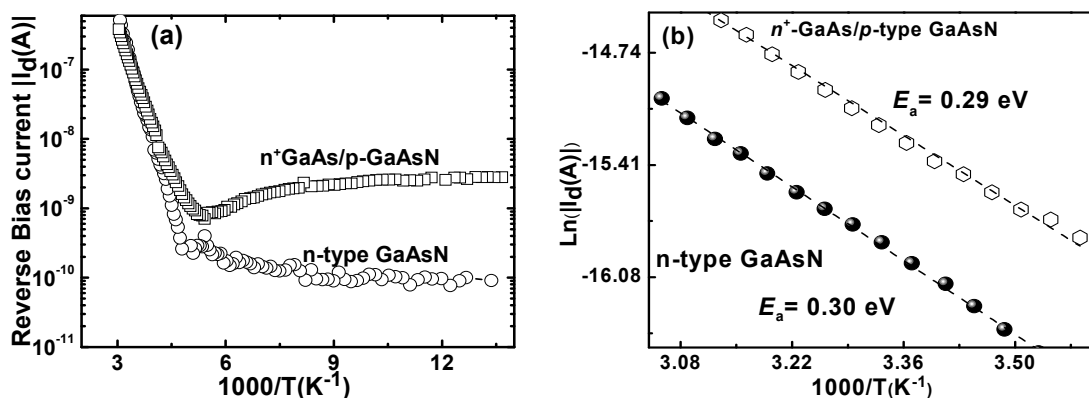


Fig. 4. Temperature dependence of dark current under reverse bias voltages of (a) 0.5 and -0.5V and (b) 1 and -1V in n -type GaAsN schottky junction and the n^+ -GaAs/ p -GaAsN heterojunction, respectively.

4.1.2.2 DC-DLTS measurements

DC-DLTS is used to confirm the recombination nature of $E1$ and to characterize the recombination process via this defect center. An unintentionally doped n -type GaAsN layer ($\sim 1 \mu\text{m}$) was grown on a p -type GaAs by CBE. This structure is not commonly used for DLTS measurements. However, the absence of a p -type doping source prevented us from obtaining a p^+ - n junction. Here, the p -type substrate is used as source of minority carriers. As shown in Fig. 5(a), the DC-DLTS spectrum is compared with that of the conventional DLTS. A decrease in the peak height of $E1$ is observed by varying the voltage of the second injected pulse and also confirmed by varying its duration. The obvious reason for such reduction is the mechanism of e - h recombination at the energy level $E1$ in the forbidden gap of GaAsN. Hence, $E1$ is reconfirmed to act as a N -related recombination center. To verify the non-radiative recombination process, the temperature dependence of σ_{E1} is obtained by varying the emission rate window e_{rw} from 0.5 - 50 s^{-1} . The value of σ_{E1} is obtained from the fitting of the Arrhenius plots for each e_{rw} . As shown in Fig. 5(b), the natural logarithmic of σ_{E1} shows a linear increase with the reciprocal of the temperature. It can be expressed as

$$\ln(\sigma_{E1}) = -E_{cap,e}/kT + \ln(\sigma_{\infty}) \quad (15)$$

where $E_{cap,e} = 0.13 \pm 0.02$ eV, k , T , and $\sigma_{\infty} = 1.38 \times 10^{-9}$ cm^2 denote the barrier height for the capture of electron, the Boltzmann constant, the temperature, and the capture cross section of

electrons at an infinite temperature, respectively. At room temperature, $\sigma_{E1}(300\text{ K})$ is evaluated to $\sim 8.89 \times 10^{-12}\text{ cm}^2$. Such a value is large enough to shorten the lifetime of electrons in *p*-type GaAsN. This indicates that *E1* is a strongly active recombination center at room temperature and the *e-h* recombination process is non-radiative. In addition, from the temperature dependence of σ_{E1} , the true energy depth of *E1* can be obtained by subtracting the barrier height for electron capture from the thermal activation energy obtained from the Arrhenius plot. The recombination center *E1* is localized at $E_a(E1) = 0.20 \pm 0.02\text{ eV}$ from the CBM of GaAsN. Furthermore, the average capture cross section of holes σ_p , at a temperature of $T = 175\text{ K}$, is estimated using Eq. 12 to be $\sigma_p(175\text{ K}) \sim 5.01 \times 10^{-18}\text{ cm}^2$. The physical parameters of *E1* can be summarized in a configuration coordinate diagram (CCD), in which the energy state of *E1* is described as a function of lattice configuration (*Q*). As shown in Fig. 5(c), the CCD of *E1* can be presented in three different branches: (i)[0, f.e + f.h]: the charge state of *E1* is neutral, with a free electron and a free hole, (ii)[- , t.e + f.h]: the electron is trapped and the hole remains free, (iii)[0]: the free hole is captured at the crossed point B and recombined with the already-trapped electron. *E1* losses its charge and becomes neutral. As the recombination process is non-radiative, the lattice relaxation occurs with the emission of multi-phonon. The energy of multi-phonon emission can be evaluated as function of *N* concentration according to

$$E_{\text{phonon}}(N) = E_g(N) - (E_a(E1) - E_{\text{cap},e}) \quad (16)$$

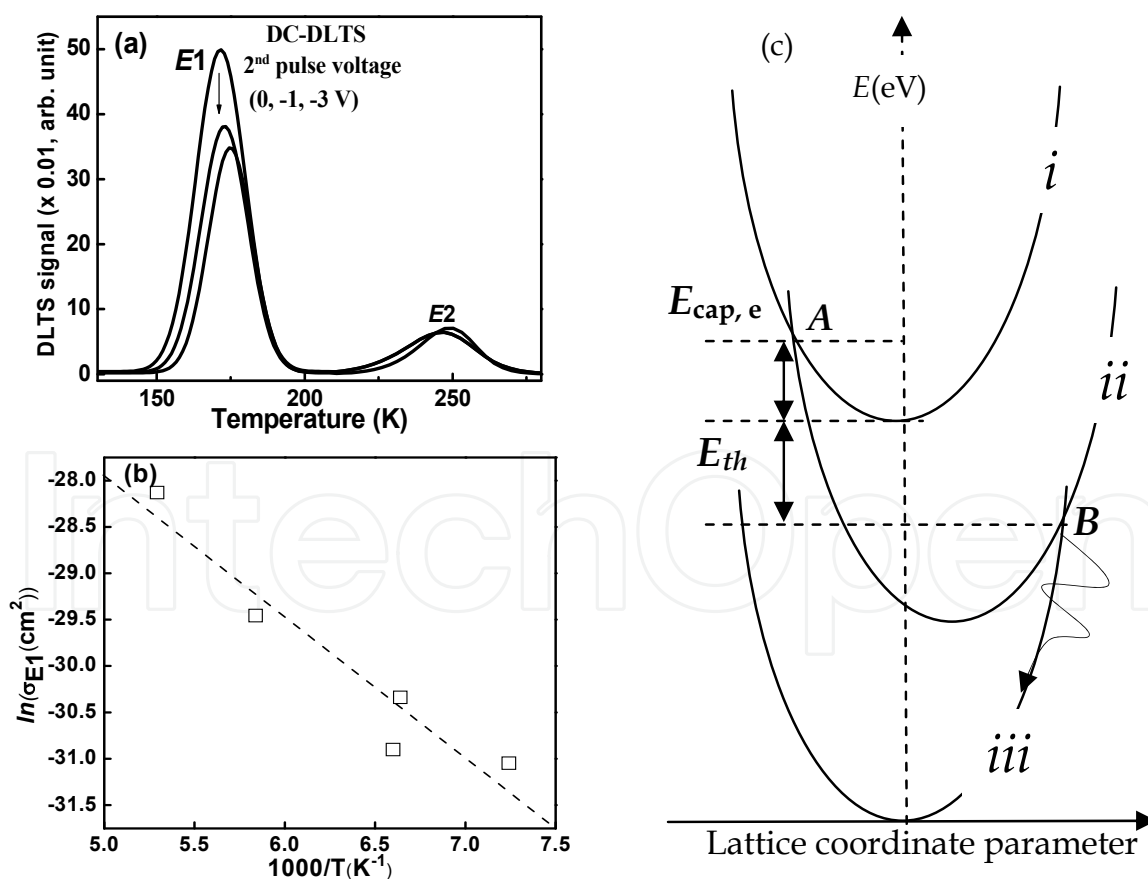


Fig. 5. (a) Reduction of peak height of *E1* under minority carrier injection spectra, (b) temperature dependence of σ_{E1} for electrons, and (c) Configuration-coordinate-diagram showing the different charge states of *E1* as function of lattice coordinate parameter.

4.1.3 Possible origin of the N-related recombination center E1

It is worth remembering that the atomic structure of $E1$ may be free from impurities and doping atoms owing to the difference in the density of residual impurities in GaAsN grown with MOCVD, MBE, and CBE. Furthermore, the uniform distribution of N_{E1} in the bulk of GaAsN indicates that $E1$ is formed during growth to compensate for the tensile strain caused by the small atomic size of N compared with that of As. Therefore, the origin of $E1$ has high probability to depend only on the atoms of the alloy (N, As, Ga). To confirm these expectations, the origin of $E1$ is investigated qualitatively by considering the results of two different experiments: (i) the dependence of N_{E1} to the As source flow rate and (ii) the effect of H implantation on the distribution of lattice defects in n -type GaAsN.

4.1.3.1 Dependence of N_{E1} to As source flow rates

The objective of this experiment is to clarify whether the density of $E1$ is sensitive to the As atom or not. The MMHy was supplied to 9.0 sccm and the TDMAAs was varied between 0.7 and 1.5 sccm. As shown in Fig. 6. (a), increasing TDMAAs drops the N concentration in the film and tends to saturate for a flow rate higher than 1 sccm. For two emission rate $e_{rw} = \{100, 10\} \text{ s}^{-1}$ and filling pulse $t_p = \{0.1, 5\} \text{ ms}$ values, the DLTS spectra are normalized on the junction capacitance to exclude the effect of various carrier densities in the samples. The same N-related recombination center $E1$ was observed in all samples. The TDMAAs flow rate dependence of the DLTS peak height of $E1$ for two settings of measurement parameters is given in Fig. 6(b). A peaking behavior at approximately TDMAAs = 0.9 sccm was obtained. As N_{E1} is uniformly distributed in GaAsN films, the incorporation of N atom at the growth surface affects both the incorporation of N_{As} and the formation of $E1$. If $E1$ depends only on N atom, the decrease of $[N]$ with increasing TDMAAs flow rate results in monotonically dropping of N_{E1} . However, the peaking behavior of N_{E1} indicates the sensitivity of $E1$ to As atom, either than N.

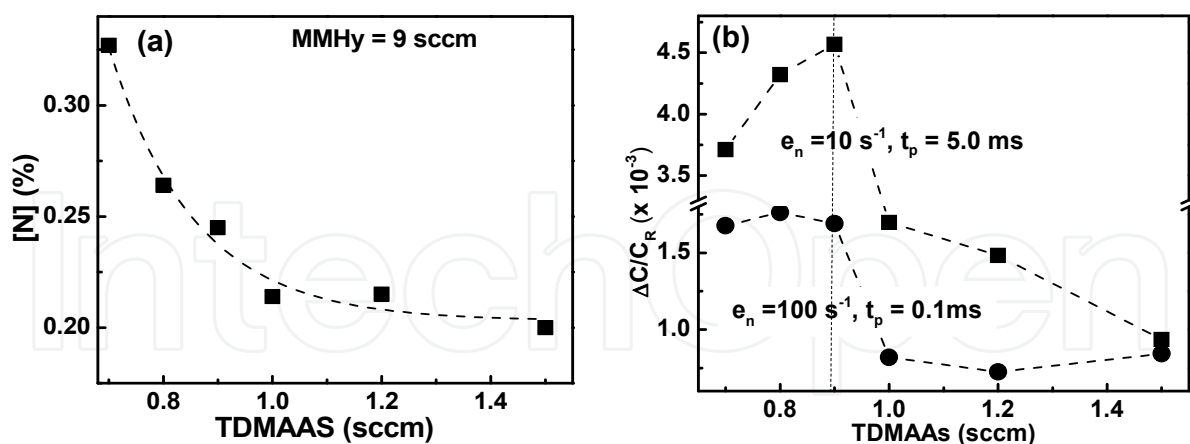


Fig. 6. TDMAAs flow rate dependence of (a) N concentration under supplied MMHy and (b) normalized DLTS peak height of $E1$ for two settings of measurement parameters.

4.1.3.2 Effect of H implantation on lattice defects in GaAsN

GaAsN films were treated by H implantation. This experiment was used because H binds strongly to N in GaAsN films to form $N-H$ complexes (Suzuki et al., 2008; Amore & Filippone, 2005). H ions with multi-energy from 10 to 48 keV were implanted into GaAsN layers with peaks concentration of 5×10^{18} ($\text{GaAsN}_{\text{HD1}}$) and 1×10^{19} atom/ cm^3 ($\text{GaAsN}_{\text{HD2}}$),

respectively. The depth of implantation was thought to be distributed between 110 and 410 nm from the surface of GaAsN by calculating the SRIM 2003 simulation code (Ziegler, 1985). After implantation, the samples were treated by post thermal annealing at 500 °C for 10 min under N₂ gas and GaAs cap layers. As plotted in Fig. 7(a) and (b), the crystal quality of GaAsN films after implantation was controlled using XRD curves and C-V measurements. DLTS spectra of implanted samples are shown in Fig. 7(c). After implantation, E1 was not observed; however, two new lattice defects appeared. The signature and the density of these traps are summarized in Table 1. The thermal emission from them is plotted as an Arrhenius plot in Fig. 7(d).

GaAsN	Traps	E _a (eV)	σ(cm ²)	N _{t-adj} (cm ⁻³)	Possible origin
As grown	E1	E _{CM} -0.331	5.18 × 10 ⁻¹⁵	3.37 × 10 ¹⁷	(N-As) _{As}
Implanted	EP1	E _{CM} -0.414	8.20 × 10 ⁻¹³	5.88 × 10 ¹⁷	EL5 in GaAs
	HP1	E _{VM} -0.105	5.42 × 10 ⁻¹⁸	1.84 × 10 ¹⁶	N-H-V _{Ga}

Table 1. Summary of E_a, σ, adjusted N_{t-adj} and possible origin of defects in as grown and implanted GaAsN samples.

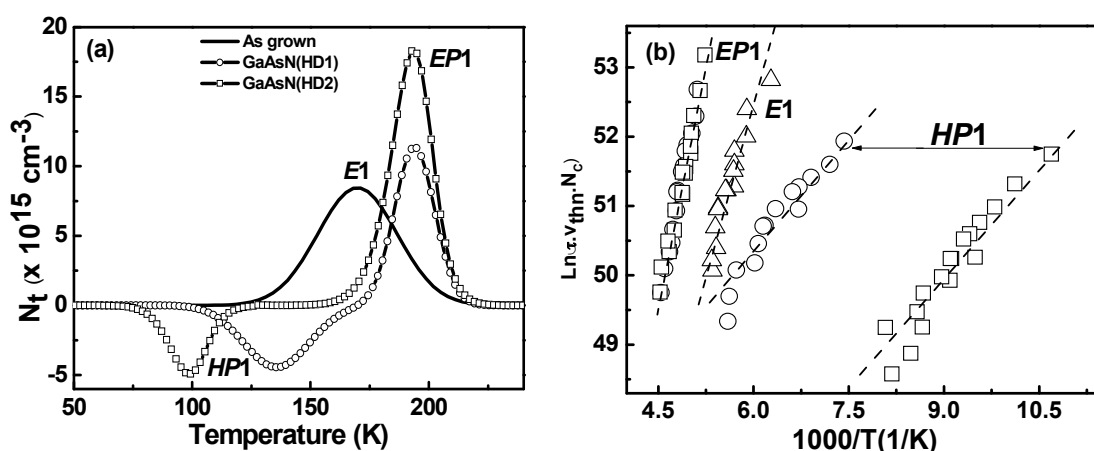


Fig. 7. (a) DLTS spectra of as grown and implanted GaAsN and (b) their Arrhenius plots.

The new electron trap (EP1) is located approximately 0.41 eV below the CBM of GaAsN. Its properties are identical to that of the native defect EL5 in GaAs (Reddy, 1996). Its atomic structure was discussed in many publications, where the common result indicated that EL5 is a complex defect free from impurities and dominated by As interstitials, such as V_{Ga}-As_i or As_{Ga}-V_{Ga} (Deenapanray et al., 2000; Yakimova et al., 1993). The second new defect is a hole trap (HP1) at approximately an average activation energy 0.11 eV above the VBM of GaAsN. Compared with majority carrier traps in GaAs grown with various techniques, no similar hole trap to HP1 was reported. However, in *p*-type GaAsN grown by CBE with around the same N concentration, E_{HP1} and σ_{HP1} are identical to that of the hole trap HC2 in *p*-type GaAsN grown by CBE (bouzazi et al., 2011). This defect was confirmed recently to be an acceptor state in GaAsN films (see § 4.2.3) and to be related to the N-H bond. While the H impurity was provided by implantation, the N atom can originate through two possibilities: First; examining XRD results, the N atom can originate from its ideal site. However, [N] in as grown is much higher than that in implanted samples (~10¹⁹ cm⁻³). It is also much higher than N_{HP1}. Second, N atom can be originated from the complete dissociation of E1, since the

ratio N_{E1}/N_{HP1} is less than 2. If $E1$ is the split interstitial $(N-N)_{As}$, N_{HP1} must be at least equals to that of $E1$ and one N atom remains free. This expectation is disapproved by DLTS measurements, where N_{HP1} is largely less than N_{E1} . This means that $E1$ contains only one N atom in its atomic structure. Considering the results of last sub-section, $E1$ may be the split interstitial $(N-As)_{As}$ formed from one N and one As in a single As site. This result is supported by the theoretical calculation (Zhang et al., 2001).

4.1.4 Effect of E1 on minority carrier lifetime in GaAsN

The effect of $E1$ on the electrical properties of GaAsN can be evaluated through the calculation of minority carrier lifetime using the SRH model for generation–recombination (Hall, 1952; Shockley & Read, 1952). Such parameter has been estimated to be less than 0.2 ns as a result of the calculation according to

$$\tau_{E1} = (v_{th} \sigma_{E1} N_{E1})^{-1} < 0.2 \text{ ns} \quad (17)$$

Therefore, $E1$ is considered to be the main cause of short minority carrier in GaAsN. It is required to investigate the formation mechanism of this defect in order to decrease its density and to recover the minority carrier lifetime in GaAs.

4.2 Hole traps in GaAsN grown by CBE

4.2.1 DLTS spectra and properties of hole traps in GaAsN

Here, we only focus on the hole traps that coexist in all p -type GaAsN based Schottky junctions and n^+ -GaAs/ p -GaAsN heterojunction. The difference between these two structures is the temperature range in which the DLTS measurements can be carried out due to the freeze-out of carriers. The DLTS spectrum of p -type GaAsN in the heterojunction is shown in Fig. 8(a). Three hole traps $H0$, $H2$, and $H5$ are observed at 0.052, 0.185, and 0.662 eV above the VBM of GaAsN. Their peak temperatures are 35, 130, and 300 K, respectively. The thermal dependence of emission from the hole traps is plotted as an Arrhenius plot in Fig. 8(b). The activation energy, capture cross section, and density are given in Table 2.

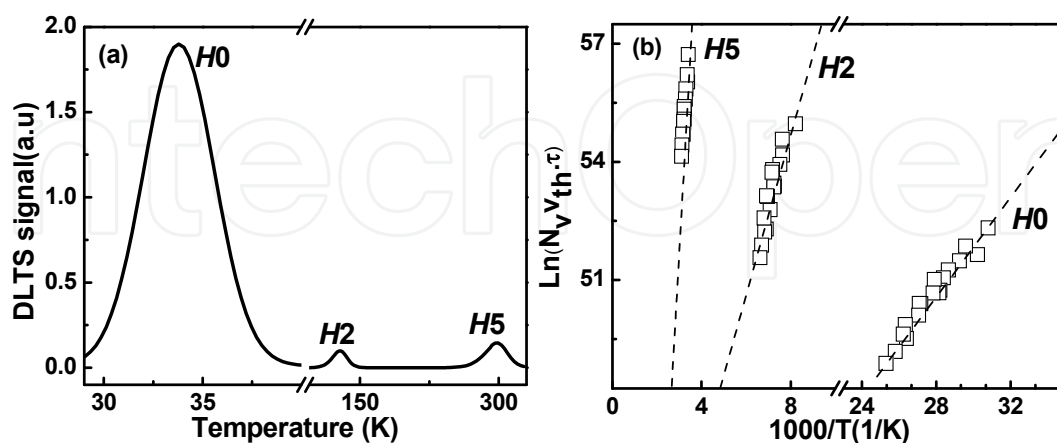


Fig. 8. (a) DLTS spectra of p -type GaAsN grown by CBE and (b) their Arrhenius plots.

The hole traps $H2$ and $H5$ were also observed in Schottky junctions and coexist in all samples. $H2$ is a N-related acceptor-like state and was proved to be in good relationship with high background doping in GaAsN films. These properties will be discussed later. The

hole trap *H5* presents the same properties as *H3* and *HA5* (Li et al., 2001; Katsuhata et al., 1978). It is proposed to be the double donor state (+/++) of *EL2* (Bouzazi et al., 2010). The hole trap *H0* cannot be observed in Schottky junctions owing to the freeze-out effect.

Traps	E_t (eV)	σ_p (cm ²)	N_{t-adj} (cm ⁻³)
<i>H0</i>	0.052	2.16×10^{-14}	4.64×10^{16}
<i>H2</i>	0.185	3.87×10^{-17}	4.52×10^{15}
<i>H5</i>	0.662	6.16×10^{-14}	6.24×10^{15}

Table 2. Summary of E_t , σ_p , and adjusted N_{t-adj} of *H0*, *H2*, and *H5*.

4.2.2 Radiative shallow recombination center *H0*

DC-DLTS measurements were carried out to confirm whether there is a recombination center among the hole traps or not. As shown in Figs. 9(a) and (b), the DC-DLTS signal is compared to that of conventional DLTS. A decrease in the DLTS peak height of *H0* is observed and confirmed by varying the voltage and the duration of the injected pulse.

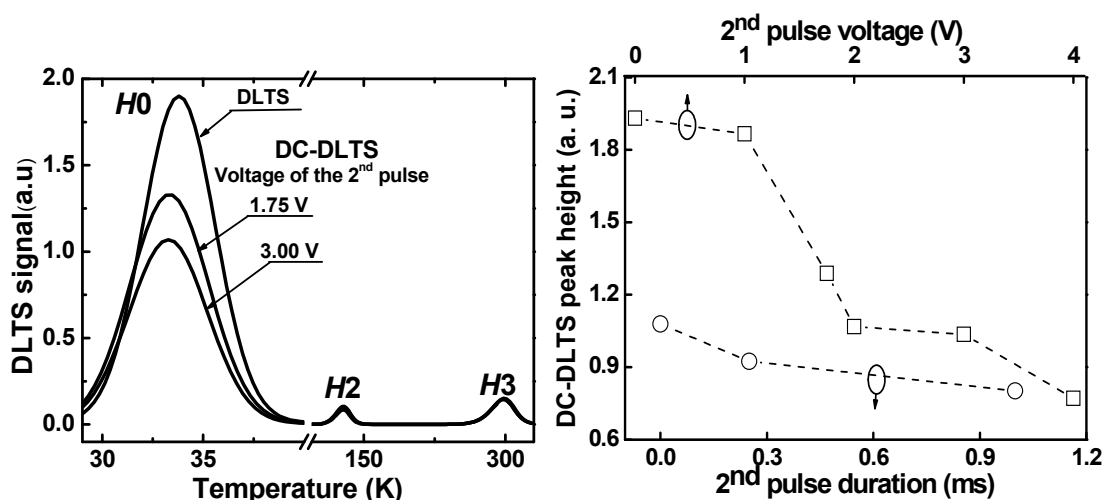


Fig. 9. (a) DC-DLTS spectra of p-type GaAsN for various second pulse voltage and (b) *H0* DC-DLTS peak height dependence of second pulse voltage and duration.

The shallow hole trap *H0* is observed and reported for the first time owing to the temperature range it was recorded, which cannot be reached with standard DLTS systems. Second, its capture cross section is large enough to capture majority carriers and minority carriers. The reduction in the peak height of *H0* is explained by the electron hole-recombination. This implies that *H0* is a shallow recombination center in p-type GaAsN grown by CBE and can also play the role of an acceptor state. To verify whether the recombination process via *H0* is radiative or not, the temperature dependence of the capture cross section of electrons is obtained by varying the emission rate e_{rw} from 1 to 50 s⁻¹. As shown in Fig. 10(a), the peak temperature of *H0* shifts to high temperatures with increasing e_{rw} . The value of σ_{H0} is obtained from the fitting of the Arrhenius plots for each e_{rw} . It is important to note that the fitting errors of activation energy and capture cross section are relatively large owing to the instability of temperature in the range of measurements. As shown in Fig. 10(b), the capture cross section of *H0* does not exhibit an Arrhenius behavior, which excludes the non-radiative recombination process. Its shallow energy level suggests

that $H0$ plays the role of an intermediate center in the recombination process, with the exception that the recombination is quite often radiative.

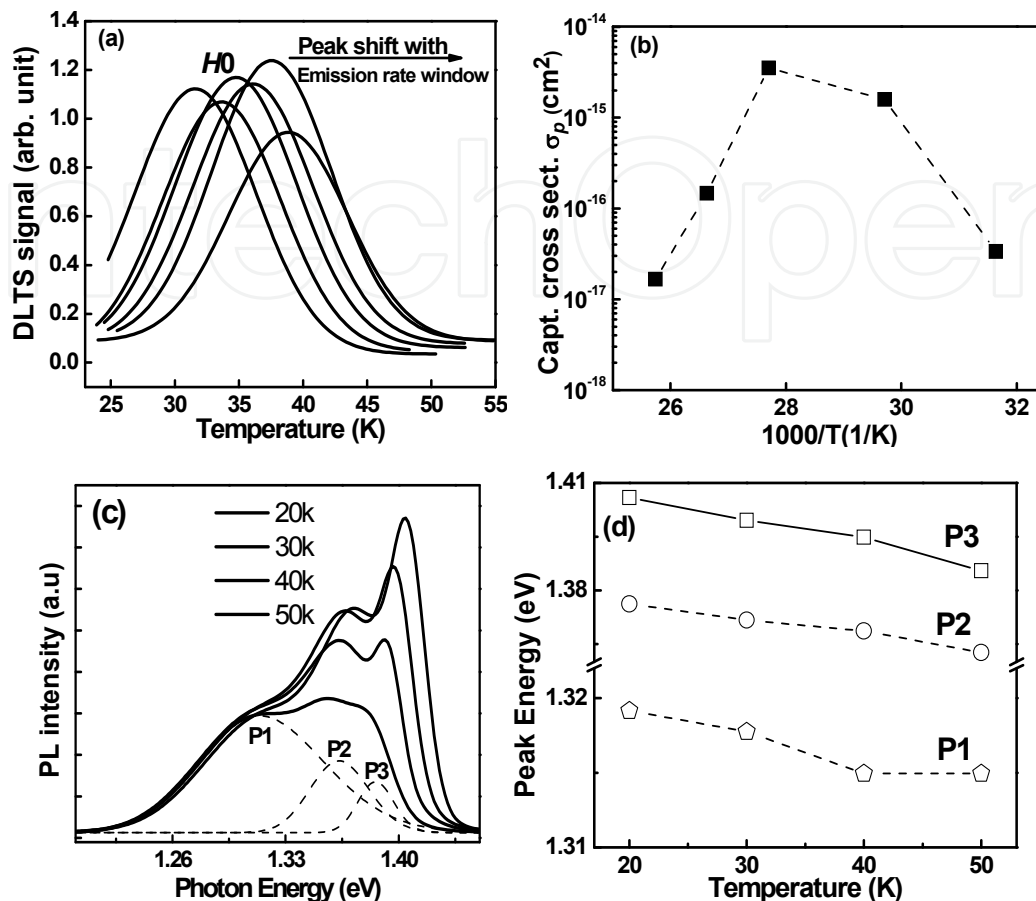


Fig. 10. (a) Emission rate window dependence of $H0$ peak, (b) temperature dependence of capture cross section and activation energy of $H0$, (c) PL spectra of p-type GaAsN at 20 to 50 K, and (d) temperature dependence of the peaks $P1$, $P2$, and $P3$ obtained from the fitting of PL spectra.

Furthermore, the capture cross section of electrons can be estimated using Eq. 13 and by the reduction of the peak height of $H0$, which follows from the injection of minority carriers. By varying the injected pulse voltage at fixed duration, the average capture cross section of electrons σ_n , at a temperature $T = 35$ K, is estimated to be $\sigma_n \sim 3.64 \times 10^{-16}$ cm². However, by varying the width of the injected pulse at fixed pulse voltage, it is estimated, at the same temperature, to be $\sigma_n \sim 3.05 \times 10^{-16}$ cm². These two values are nearly identical and indicate that the capture cross section of electrons and holes of $H0$ are approximately the same. To identify this radiative recombination, photoluminescence (PL) measurements were carried out at low temperature on the same GaAsN sample. The PL spectra at 20, 30, 40, and 50 K are shown in Fig. 10 (c). Three different peaks $P1$, $P2$, and $P3$ can be distinguished from PL spectra fitting. The temperature dependence of their energies is plotted in Fig. 10 (d). The three peaks were sufficiently discussed in many N-varying GaAsN samples and they are proposed to be: (i) $P1$ is the result of band-to-band transition, (ii) $P2$ is caused by free exciton or related to shallow energy level, and (iii) $P3$ originates from the transition between a neutral donor and a neutral acceptor pair (DAP) (Inagaki et al., 2011). Therefore, the peak $P2$

is suggested to be in relation with $H0$. The band diagram of such recombination is shown in Fig. 11, where the transition occurs between $H0$ and the CBM and/or a donor-like defect (E_t). The transition between free electrons in the CBM and charged $H0$ is called free-to-charged bound transition.

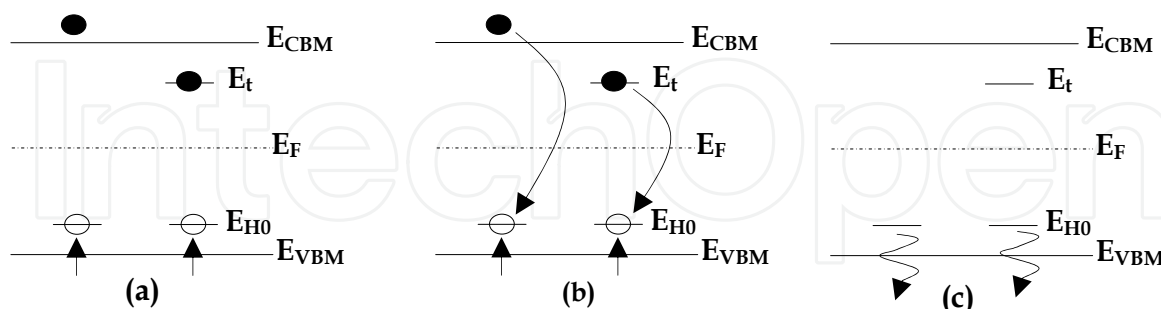


Fig. 11. Band diagram of radiative recombination through $H0$, where the transition occurs between $H0$ and the CBM and/or a donor-like defect (E_t).

Concerning the origin of the acceptor-like hole trap $H0$, more experiments are required to discuss it. However, considering its density and the distribution of shallow acceptors in GaAs, it can be suggested that $H0$ is a carbon-related acceptor, where the reported ionization energy from PL and Hall Effect measurements is 0.026 eV and its density in the 10^{-15} cm^{-3} range (Baldereschi & Lipari, 1974).

4.2.3 Deep N-H related acceptor state $H2$

The ionized acceptor density (N_A) is found to be in good linear dependence with N concentration in p -type GaAsN samples (see Fig. 12 (a)). As given in Figs. 12(b) and (c), the junction capacitance (C_j) showed a N -related sigmoid behavior with temperature in the range 70 to 100 K. This behavior has not yet been observed in GaAs and n -type GaAsN grown by CBE. It was recorded at 20 K in silicon p - n junction and explained by the ionization of a shallow energy level (Katsuhata, 1978; 1983). Hence, the N dependence of N_A and C_j is explained by the thermal ionization of a N -related acceptor-like state. The thermal ionization energy of this energy level was estimated in the temperature range 70 to 100 K to be between 0.1 and 0.2 eV. It is in conformity with the theoretical calculations, which suggested the existence of a N -related hole trap acceptor-like defect with an activation energy within 0.03 and 0.18 eV above the VBM of GaAsN (Janotti et al., 2003; Suzuki et al., 2008). Experimentally, a deep acceptor level, $A2$, was confirmed in CBE grown undoped GaAsN with ionization energies of $E_{A1} = 130 \pm 20 \text{ meV}$ (Suzuki et al., 2008). On the other hand, the properties of $H2$ in N -varying GaAsN schottky junctions are cited below: The peak temperature of $H2$ is within the temperature range of increase of C_j . This means that the electric field at this temperature range follows the same behavior of C_j and depends on N concentration. Hence, the emission of carriers from the charged traps is affected by the Poole-Frenkel emission (Johnston and Kurtz, 2006). This is confirmed by the fluctuation of E_{H2} from one sample to another depending on N concentration (see Table 3). However, the average of E_{H2} is within the energy range of the acceptor level obtained from theoretical prediction and identical to E_{A2} (Suzuki et al., 2008; Janotti et al., 2003). Furthermore, as given in Fig. 12 (d), $N_{H2\text{-adj}}$ is in linear dependence with N concentration. Therefore, $H2$ is proved to be the N -related hole trap acceptor-like state, which thermal ionization increased C_j and

drops the depletion region width. The contribution of H_2 in the background doping of p -type GaAsN films grown by CBE can be evaluated from the ratio between the real $N_{H_2-C_j}$ calculated from the change of C_j and N_A at room temperature (Bouzazi et al., 2010). As shown in Fig. 12 (e) and (f), This ratio comes closer to the unit for a N concentration greater than 0.2%. Thus, H_2 is the main cause of the high background doping in p -type GaAsN.

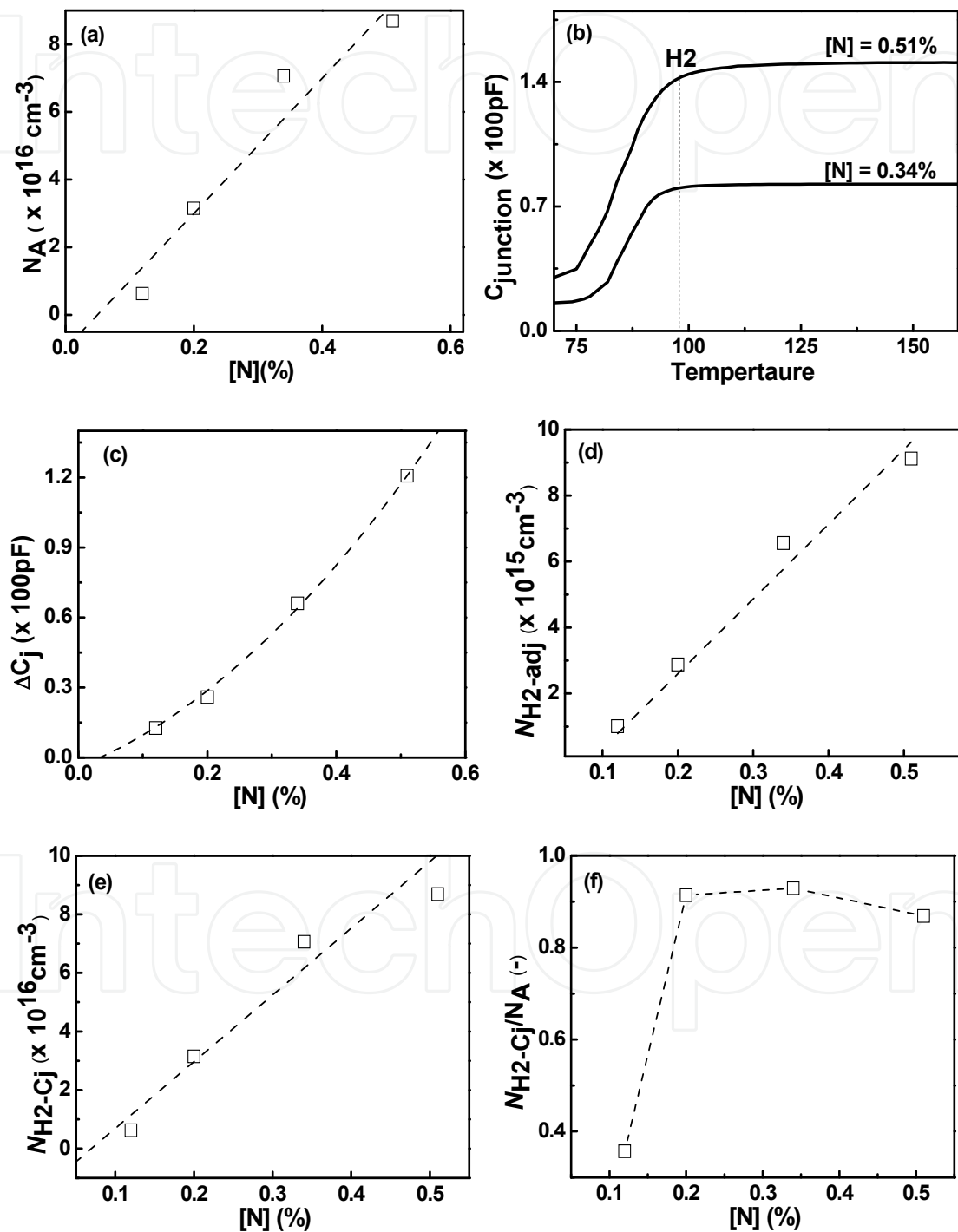


Fig. 12. N dependence of (a) N_A , (c) amplitude of C_j after thermal ionization of H_2 , and (d) $N_{H_2\text{-adj}}$. (b) Sigmoid increase of C_j between 70 and 100 K for two different GaAsN samples. N dependence of (e) $N_{H_2-C_j}$ and (f) $N_{H_2-C_j}/N_A$.

To investigate the origin of $H2$, it is worth remembering some previous results about carrier concentration and the density of residual impurities in undoped GaAsN grown by CBE, obtained using Hall Effect, Fourier transform infra-red (FTIR), and second ion mass spectroscopy (SIMS) measurements. On one hand, under lower Ga flow rates (TEGa), N_A and N_{H2} showed a rapid saturation with $[N]$, despite the increase of $[N]$ (see Fig. 13 (a)). This means that the atomic structure of $H2$ depends on other atoms, either than N . In addition, the densities of C and O was found to be less than free hole concentration, which excludes these two atoms from the origin of $H2$. On the other hand, using SIMS measurements, the ratio $[H]_{TEGa = 0.02} / [H]_{TEGa = 0.1}$ was evaluated to be ~ 0.6 (Sato et al., 2008). Furthermore, the free hole concentration at room temperature showed a linear increase with the density of $N-H$ bonds (Nishimura et al., 2006). This means that N_A depends strongly on $[H]$ and the saturation of N_A under lower TEGa can be explained by the desorption of H from the growth surface, since the growth rate in our films was found to be in linear dependence with TEGa. Hence, the structure of $H2$ is related to the $N-H$ bond. However, the $N-H$ bond may not be the exact structure of $H2$ because the slope of the linear relationship between N_A and $[N-H]$ increased with increasing growth temperature ($T_G \in [400, 430]$ °C). This indicates that N_A is determined by both the number of $N-H$ and another unknown defect, which concentration increased with increasing T_G . The binding energy of this unknown defect can be determined from Arrhenius plot. Furthermore, the formation energy of $(N-H-V_{Ga})^{-2}$ was found to be lower than $(N-V_{Ga})^{-3}$, $(H-V_{Ga})^{-2}$, and isolated V_{Ga}^{-3} (Janotti et al., 2003). This means that the unknown defect may be V_{Ga} . These predictions were experimentally supported using positron annihilation spectroscopy results (Toivonen et al., 2003). Hence, $H2$ may be related to the $N-H-V_{Ga}$ structure.

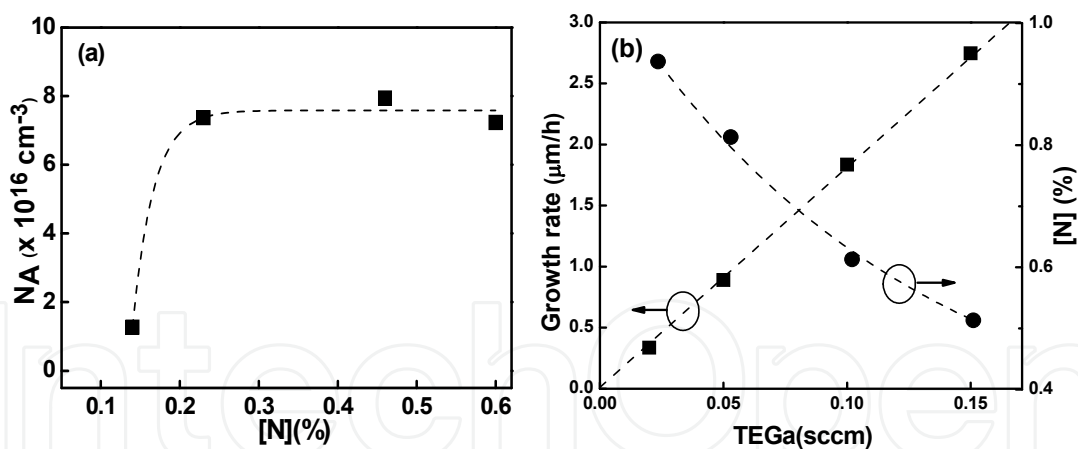


Fig. 13. N dependence of (a) N_A and (b) TEGa flow rate dependence of growth rate and N concentration at a growth temperature of 420 °C.

$[N](\%)$	E_{H2} (eV)	$\sigma_{H2}(\text{cm}^2)$	$N_{H2\text{-adj}}(\text{cm}^{-3})$	E_{max} (V/cm)	$N_{H2\text{-Cj}}(\text{cm}^{-3})$	$N_{H2\text{-Cj}}/N_A$
0.12	0.210	2.8×10^{-14}	2.64×10^{15}	6.2×10^4	2.23×10^{15}	0.36
0.20	0.150	6.3×10^{-16}	3.08×10^{15}	1.4×10^5	2.88×10^{16}	0.91
0.34	0.138	6.3×10^{-16}	5.20×10^{15}	2.1×10^5	6.56×10^{16}	0.93
0.51	0.103	1.3×10^{-17}	9.12×10^{15}	2.3×10^5	7.55×10^{16}	0.87

Table 3. Summary of E_{H2} , σ_{H2} , $N_{H2\text{-adj}}$, E_{max} , $N_{H2\text{-est}}$, and the ratio $N_{H2\text{-Cj}}/N_A$ for CBE grown undoped p -type GaAsN Schottky junctions.

5. Conclusion

Three defect centers, related to the optoelectronic properties of GaAsN, were identified and characterized using DLTS and some related methods:

- The first defect is a N-related non-radiative recombination center (*E1*), located approximately 0.33 eV below the CBM of GaAsN grown by CBE. *E1* is a stable defect and exhibits a large capture cross section at room temperature. Its activation energy comes closer to the midgap by increasing the N concentration in the film, which increases the recombination rates of carriers. In addition, the density profiling of *E1* was found to be uniformly distributed, which may indicate that this defect was formed during growth to compensate for the tensile strain caused by N. Using the SRH model for generation-recombination, the lifetime of electrons to *E1* was evaluated to be ~0.2 ns. Therefore, *E1* is suggested to be the main cause of poor minority carrier lifetime in GaAsN films. Its origin was suggested to be the split interstitial formed from one N and one As in a single arsenic site.
- The second defect is a radiative shallow hole trap acceptor-like state (*H0*), at 0.052 eV above the VBM of GaAsN. It was observed and reported for the first time in GaAs and GaAsN films. The radiative recombination process through *H0* is confirmed to be a free-to-charged bound transition. This defect may be in relationship with carrier density and the optical properties of the film.
- The last defect is a N-related hole trap acceptor-like state (*H2*) located approximately 0.15 eV above the VBM of GaAsN. It was newly observed in GaAsN films. *H2* was proved to have a good relationship with the carrier density and to be the main origin of high background doping in GaAsN films, essentially for relatively high N concentration. *H2* is strongly suggested to be related with N-H bond. Its formation limits the junction depth and minimizes the contribution of the depletion region in the quantum efficiency of GaAsN based solar cells.

In conclusion, the results obtained in this study are very useful for scientific understanding of defects in III-V-N materials and to improve GaAsN and InGaAsN qualities for realizing high efficiency multi-junction solar cells.

6. Acknowledgment

Part of this work was supported by the New Energy Development Organization (NEDO) under the Ministry of Economy, Trade and Industry, Japan.

7. References

- Ahlgren, T.; Vainonen-Ahlgren, E.; Likonen, J.; Li, W. & Pessa, M. (2002). Concentration of interstitial and substitutional nitrogen in GaN_xAs_{1-x}. Applied Physics Letters, Vol. 80, pp. 2314-2316.
- Amore, B. A. & Filippone, F. (2005). Theory of Nitrogen-Hydrogen Complexes in N-containing III-V Alloys, chapter 13, Dilute Nitride Semiconductors, Henidi, M. Elsevier Ltd, UK.
- Baldereschi, A. & Lipari, N. O. (1974). Cubic contributions to the spherical model of shallow acceptor states. Physical Review B, Vol.9, pp. 1525-1539.

- Bouzazi, B.; Nishimura, K.; Suzuki H.; Kojima, N.; Ohshita, Y. & Yamaguchi M. (2010). Properties of Chemical Beam Epitaxy grown GaAs_{0.995}N_{0.005} Homo-junction Solar Cell, *Current Applied Physics*, Vol.10, pp. 188-190.
- Bouzazi, B.; Suzuki, H.; Kojima, N.; Ohshita, Y. & Yamaguchi, M. (2011). *Japanese Journal of Applied Physics*, Vol.49, pp. 121001-121006.
- Bube, R. H. (1956). Comparison of Surface-Excited and Volume-Excited Photoconduction in Cadmium Sulfide Crystals. *Physical Review*, Vol.101, pp. 1668-1676.
- Bube, R. H. (1960). *Photoconductivity of Solids*. John Wiley & Sons, Inc., New York, pp. 292-299.
- Deenapanray, P. N. K.; Tan, H. H. & Jagadish, C. (2000). Investigation of deep levels in rapid thermally annealed SiO₂-capped n-GaAs grown by metal-organic chemical vapor deposition. *Applied Physics Letters*, Vol.77, pp. 696-698.
- DeVore, H. B. (1959). Gains, response times, and trap distributions in powder photoconductors. *RCA Review*, Vol. 20, pp. 79-91.
- Friedman, D. J.; Geisz, J. F.; Kurtz, S. R.; & Olson, J. M. (1998). 1-eV Solar Cells with GaInNAs Active Layer. *Journal of Crystal Growth*, Vol.195, pp. 409-415.
- Geisz, J. F.; Friedman, D. J.; Olson, J. M.; Kurtz, S. & Keyes, B. M. (1998). Photocurrent of 1 eV GaInNAs lattice-matched to GaAs. *Journal of Crystal Growth*, Vol.195, pp. 401-408.
- Geisz, J. F. & Friedman, D. J. (2002). III-N-V Semiconductors for Solar Photovoltaic Applications. *Semiconductor Science and Technology*, Vol.17, No.8, pp. 769-777.
- Hall, R. N. (1952). Electron-Hole Recombination in Germanium. *Physical Review*, Vol. 87, pp. 387-387.
- Inagaki, M.; Suzuki, H.; Suzuki, A.; Mutaguchi, K.; Fukuyama, A.; Kojima, N.; Ohshita, Y. & Yamaguchi, M. (2011). Shallow Carrier Trap Levels in GaAsN Investigated by Photoluminescence. *Japanese Journal of Applied Physics*, Vol.50, 4, pp. 04DP141-144.
- Janotti, A.; Zhang, S. B.; Wei, S. H. & Van de Walle, C. G. (2002). Effects of hydrogen on the electronic properties of dilute GaAsN alloys. *Physical Review Letters*, Vol.89, pp. 6403-6406.
- Janotti, A.; Wei, S. H.; Zhang, S. B. & Kurtz, S. (2003). Interactions between nitrogen, hydrogen, and gallium vacancies in GaAs_{1-x}N_x alloys. *Physical Review B*, Vol.67, pp. 161201-161204.
- Jock, M. R. (2009). Effect of N Interstitials on the Electronic Properties of GaAsN Alloy Films. Thesis, the University of Michigan, 2009.
- Johnston, S. W. & Kurtz, S. R. (2006). Comparison of a dominant electron trap in *n*-type and *p*-type GaNAs using deep-level transient spectroscopy. *Journal of Vacuum Science & Technology*, A24 (4), pp. 1252-1257.
- Katsuhata, M.; Koura, K. & Yoshida S. (1978). Temperature Dependence of Capacitance of Silicon p-n Step Junctions. *Japanese Journal of applied physics*, Vol.17, pp. 2063-2064.
- Katsuhata, M.; Yamagata, S., Miyayama, Y.; Hariu, T. & Shibata, Y. (1983). P-n Junction Capacitance Thermometers. *Japanese Journal of Applied Physics*, Vol.22, pp. 878-881.

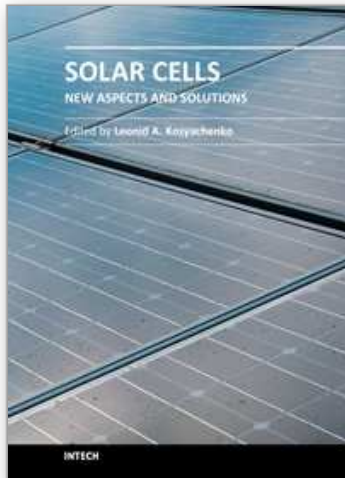
- Krispin, P.; Spruytte, S. G.; Harris, J. S. & Ploog, K. H. (2000). Electrical depth profile of p-type GaAs/Ga(As, N)/GaAs hetero-structures determined by capacitance-voltage measurements. *Journal of Applied Physics*, Vol.88, pp. 4153- 4158.
- Krispin P.; Gambin V.; Harris J. S. & Ploog K. H. (2003). Nitrogen-related electron traps in Ga(As,N) layers (< 3% N). *Journal of Applied Physics*, Vol.93, pp. 6095-6099.
- Krispin, P.; Spruytte, S. G.; Harris, J. S. & Ploog, K. H. (2001). Origin and annealing of deep-level defects in p-type GaAs/Ga(As,N)/GaAs hetero-structures grown by molecular beam epitaxy. *Journal of Applied Physics*, Vol.89, pp. 6294-6301.
- Kurtz, S.; Allerman, A. A.; Jones, E. D.; Gee, J. M.; Banas, J. J. & Hammons, B. E. (1999). InGaAsN solar cells with 1.0 eV band gap, lattice matched to GaAs. *Applied Physics Letters* Vol.74, pp. 729-731.
- Kurtz, S.; Webb, J.; Gedvilas, L.; Friedman, D.; Geisz, J.; Olson, J.; King, R., Joslin, D. & Karam, N. (2001). Structural changes during annealing of GaInAsN. *Applied Physics Letters*, Vol.78, pp. 748-750.
- Kurtz, S.; Reedy, R.; Barber, G. D.; Geisz, J. F.; Friedman, D. J.; McMahon, W. E. & Olson, J. M. (2002) Incorporation of nitrogen into GaAsN grown by MOCVD using different precursors. *Journal of Crystal Growth*, Vol.234, pp. 318-322.
- Kurtz, S. R.; Geisz, J. F.; Keyes, B. M.; Metzger, W. K.; Friedman, D. J.; Olson, J. M.; King, R. R. & Karam, N. H. (2003). Effect of growth rate and gallium source on GaAsN. *Applied Physics Letters*, Vol.82, pp. 2634-2636.
- Lambe, J. (1955). Recombination Processes in Cadmium Sulfide. *Physical Review*, Vol.98, pp. 985-992.
- Lampert, M. A. (1956). Simplified Theory of Space-Charge-Limited Currents in an Insulator with Traps, *Physical Review*, Vol.103, pp. 1648-1656.
- Lang, D. V. (1974). Deep-level transient spectroscopy: A new method to characterize traps in semiconductors. *Journal of applied Physics*, Vol.45, pp.3023-3032.
- Lee, H. S.; Nishimura, K.; Yagi, Y.; Tachibana, M.; Ekins-Daukes, N. J.; Ohshita, Y.; Kojima, N.; Yamaguchi, M. (2005). Chemical beam epitaxy of InGaAsN films for multi-junction tandem solar cells. *Journal of Crystal Growth*, Vol.275, pp. 1127-1130.
- Leonard, I. & Grossweiner, A. (1953). A Note on the Analysis of First-Order Glow Curves. *Journal of Applied Physics*, Vol.24, pp. 1306-1307.
- Li, J. Z.; Lin, J. Y.; Jiang, H. X.; Geisz, J. F. & Kurtz, S. R. (1999). Persistent photoconductivity in $\text{Ga}_{1-x}\text{In}_x\text{N}_y\text{As}_{1-y}$. *Applied Physics Letters*, Vol.75, pp. 1899-1901.
- Li, W.; Pessa, M.; Ahlgren, T.; & Dekker, J. (2001). Origin of improved luminescence efficiency after annealing of Ga(In)NAs materials grown by molecular-beam epitaxy. *Applied Physics Letters*, Vol.79, pp. 1094-1096.
- Losee, D. L. (1974). Admittance spectroscopy of deep impurity levels: ZnTe Schottky barriers. *Applied Physics Letters*, Vol.21, pp. 54-56.
- Moto, A.; Takahashi, M. & Takagishi, S. (2000). Hydrogen and carbon incorporation in GaInNAs. *Journal of Crystal Growth*, Vol.221, pp. 485-490.

- Nishimura, K.; Suzuki, H.; Saito, K.; Ohshita, Y.; Kojima, N. & Yamaguchi, M. (2007). Electrical properties of GaAsN film grown by chemical beam epitaxy. *Physica B*, Vol.401, pp. 343-346.
- Reddy, C. V.; Fung, S. & Beling, C. D. (1996). Nature of the bulk defects in GaAs through high-temperature quenching studies. *Physical Review B*, 54, pp. 11290-11297.
- Rose, A. (1951). An outline of some photoconductive processes. *RCA Review.*, Vol.12, pp. 362-414.
- Rose, A. (1955). Space-Charge-Limited Currents in Solids. *Physical Review*, Vol.97, pp. 1538-1544.
- Saito K.; Nishimura K.; Suzuki H.; Kojima N.; Ohshita Y. & Yamaguchi, M. (2008). Hydrogen reduction in GaAsN thin films by flow rate modulated chemical beam epitaxy. *Thin Solid Films*, Vol.516, pp. 3517-3520.
- Sah, C. T.; Chan, W. W.; Fu, H. S. & Walker, J. W. (1972). Thermally Stimulated Capacitance (TSCAP) in p-n Junctions. *Applied Physics Letters*, Vol.20, pp. 193-195
- Sah, C. T. & Walker, J. W. (1973). Thermally stimulated capacitance for shallow majority-carrier traps in the edge region of semiconductor junctions. *Applied Physics Letters*, Vol.22, pp. 384-385.
- Shockley, W. & Read, W.T. (1952). Statistics of the Recombinations of Holes and Electrons. *Physical Review*, Vol. 87, pp. 835-842.
- Smith, R. W. & Rose, A. (1955). Space-Charge-Limited Currents in Single Crystals of Cadmium Sulfide. *Physical Review*, Vol.97, pp. 1531-1537.
- Spruytte, S. G.; Coldren, C. W.; Harris, J. S.; Wampler, W.; Ploog, K. & Larson, M. C. (2001). Incorporation of nitrogen in nitride-arsenides: Origin of improved luminescence efficiency after anneal. *Journal of Applied Physics*, Vol.89, pp. 4401-4406.
- Suzuki, H.; Nishimura, K.; Saito, K.; Hashiguchi, T.; Ohshita, Y.; Kojima, N. & Yamaguchi, M. (2008). Effects of Residual Carbon and Hydrogen Atoms on Electrical Property of GaAsN Films Grown by Chemical Beam Epitaxy. *Japanese Journal of Applied Physics*, Vol.47, pp. 6910-6913.
- Toivonen, J.; Hakkarainen, T.; Sopanen, M.; Lipsanen, H.; Oila, J. & Saarinen, K. (2003). Observation of defect complexes containing Ga vacancies in GaAsN. *Applied Physics Letters*, Vol.82, pp. 40-43.
- Williams, R. (1966). Determination of Deep Centers in Conducting Gallium Arsenide. *Journal of Applied Physics*, Vol.37, pp. 3411-3416.
- Yakimova, R.; Paskova, T. & Hardalov, Ch. (1993). Behavior of an EL5-like defect in metalorganic vapor-phase epitaxial GaAs:Sb. *Journal of Applied Physics*, Vol.74, pp. 6170-6173.
- Yamaguchi, M.; Warabisako, T.; Sugiura, H. (1994). Chemical beam epitaxy as a breakthrough technology for photovoltaic solar energy applications. *Journal of Crystal Growth*, Vol.136, pp.29-36.
- Zhang, S. B. & Wei, S. H. (2001). Nitrogen Solubility and Induced Defect Complexes in Epitaxial GaAs:N. *Physical Review Letters*, Vol.86, pp. 1789-1792.

Ziegler, J. F.; Biersack J. P. & U. Littmark. (1985). The Stopping and Ion Range of Ions in Solids. Pergamon, New York, Vol. 1; SRIM program for PCs available from J. F. Ziegler and: www.srim.org.

IntechOpen

IntechOpen



Solar Cells - New Aspects and Solutions

Edited by Prof. Leonid A. Kosyachenko

ISBN 978-953-307-761-1

Hard cover, 512 pages

Publisher InTech

Published online 02, November, 2011

Published in print edition November, 2011

The fourth book of the four-volume edition of 'Solar cells' consists chapters that are general in nature and not related specifically to the so-called photovoltaic generations, novel scientific ideas and technical solutions, which has not properly approved. General issues of the efficiency of solar cell and through hydrogen production in photoelectrochemical solar cell are discussed. Considerable attention is paid to the quantum-size effects in solar cells both in general and on specific examples of super-lattices, quantum dots, etc. New materials, such as cuprous oxide as an active material for solar cells, AlSb for use as an absorber layer in p-i-n junction solar cells, InGaAsN as a promising material for multi-junction tandem solar cells, InP in solar cells with MIS structures are discussed. Several chapters are devoted to the analysis of both status and perspective of organic photovoltaics such as polymer/fullerene solar cells, poly(p-phenylene-vinylene) derivatives, photovoltaic textiles, photovoltaic fibers, etc.

How to reference

In order to correctly reference this scholarly work, feel free to copy and paste the following:

Boussairi Bouzazi, Hidetoshi Suzuki, Nobuaki Kijima, Yoshio Ohshita and Masafumi Yamaguchi (2011). Investigation of Lattice Defects in GaAsN Grown by Chemical Beam Epitaxy Using Deep Level Transient Spectroscopy, *Solar Cells - New Aspects and Solutions*, Prof. Leonid A. Kosyachenko (Ed.), ISBN: 978-953-307-761-1, InTech, Available from: [http://www.intechopen.com/books/solar-cells-new-aspects-and-solutions/investigation-of-lattice-defects-in-gaasn-grown-by-chemical-beam-epitaxy-using-deep-level-transient-](http://www.intechopen.com/books/solar-cells-new-aspects-and-solutions/investigation-of-lattice-defects-in-gaasn-grown-by-chemical-beam-epitaxy-using-deep-level-transient)

INTECH
open science | open minds

InTech Europe

University Campus STeP Ri
Slavka Krautzeka 83/A
51000 Rijeka, Croatia
Phone: +385 (51) 770 447
Fax: +385 (51) 686 166
www.intechopen.com

InTech China

Unit 405, Office Block, Hotel Equatorial Shanghai
No.65, Yan An Road (West), Shanghai, 200040, China
中国上海市延安西路65号上海国际贵都大饭店办公楼405单元
Phone: +86-21-62489820
Fax: +86-21-62489821

© 2011 The Author(s). Licensee IntechOpen. This is an open access article distributed under the terms of the [Creative Commons Attribution 3.0 License](#), which permits unrestricted use, distribution, and reproduction in any medium, provided the original work is properly cited.

IntechOpen

IntechOpen